

DEFORMER: Coupling Deformed Localized Patterns with Global Context for Robust End-to-end Speech Recognition

Jiamin Xie¹, John H.L. Hansen¹

¹ Center for Robust Speech Systems (CRSS), University of Texas at Dallas, TX, 75080

{Jiamin.Xie, John.Hansen}@utdallas.edu

Abstract

Convolutional neural networks (CNN) have improved speech recognition performance greatly by exploiting localized time-frequency patterns. But these patterns are assumed to appear in symmetric and rigid kernels by the conventional CNN operation. It motivates the question: What about asymmetric kernels? In this study, we illustrate adaptive views can discover local features which couple better with attention than fixed views of the input. We replace depthwise CNNs in the Conformer architecture with a deformable counterpart, dubbed this “Deformer”. By analyzing our best-performing model, we visualize both local receptive fields and global attention maps learned by the Deformer and show increased feature associations on the utterance level. The statistical analysis of learned kernel offsets provides an insight into the change of information in features with the network depth. Finally, replacing only half of the layers in the encoder, the Deformer improves +5.6% relative WER without a LM and +6.4% relative WER with a LM over the Conformer baseline on the WSJ *eval92* set.

Index Terms: Deformable CNN, Conformer, End-to-end Speech Recognition

1. Introduction

Convolution neural networks (CNN) are widely used to process signals generated in various domains, including images [1, 2, 3], languages [4, 5, 6], and sounds [7, 8, 9]. The basic operation of the CNN computes a weighted sum of the input within a kernel. The kernel shape is defined by the kernel size and dilation parameter, which controls the gap between consecutive positions inside a kernel. For example, a grid-like kernel has dilation of 1. The kernel sweeps the input signal yielding output at each location sequentially. Different from the convolution used in signal processing [10, 11], the CNN uses learnable filters and does not flip the input. Modern methods stem from the basic CNN operation, including dynamic convolution [12], separable convolution [13], differential strides [14], etc. The kernel shape, however, is commonly kept symmetric and rigid.

In speech recognition, CNNs are applied directly or modified for both acoustic modeling in hybrid systems and end-to-end (E2E) systems. In [15, 16], multiple streams of CNNs with varying dilation rates and kernel sizes were combined to extract acoustic features at different input resolutions. For E2E systems, the VGG-like convolutional network is one popular choice used to subsample and encode speech [17, 18]. In [19], a multi-encoder structure takes further advantage of architectural differences in addition to multi-resolution. Recent advancements are inspired by works in the vision community. QuartzNet [20] reduces model parameters using separable convolution [13]. ContextNet [21] utilizes squeeze-and-excitation [13] to channel-wise modulate the output by pooling a global context from the full utterance. The Conformer architecture

[22] further integrates both convolution and attention [23] to couple both local and global relationships, which is found to be useful in many speech related tasks [24, 25].

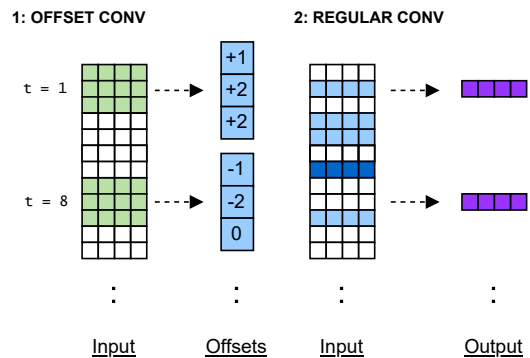


Figure 1: Deformable convolution steps, shown with kernel size=3, stride=7, dilation=1. Note at $t=8$, the kernel positions become overlapped after the offset operation.

The wide use of CNNs in speech recognition systems suggests the importance of localized patterns. One speech recording can capture both task-relevant and task-irrelevant information (e.g. speech and speaker vs. noise and channel). But all regions are scanned and processed *equally* when a convolution kernel slides across the input audio. This weakens a model’s capacity to capture localized patterns because the kernel weights have to adjust and de-emphasize irrelevant contents. Thus, if a model can constantly adapt to the input by predicting task-relevant regions, the convolution can learn better weights to strengthen the information in a local context. This fundamental problem is considered using the deformable CNN [26], originally proposed to operate on 2-D input for image segmentation tasks. In [27], the 1-D version is first used for speech recognition. The idea was to scan the input and predict offsets that deform the kernels in a subsequent convolution. As illustrated in Fig. 1, one deformable convolution consists of an offset CNN and an output CNN. Similar to CNNs, the deformable CNN employs parameters such as kernel size, stride, and dilation. But unlike conventional CNNs, the hyperparameters only specify the input sequence locations of the offset CNN. The input sequence locations of the output CNN are deformed by the predicted offsets. Therefore, a deformable CNN can help build localized patterns by focusing on the most relevant information.

In this study, we present a novel encoder model called Deformer to learn deformed localized patterns. We introduce the deformable variant of the depthwise CNN that the encoder uses. Lastly, we provide an in-depth analysis of the patterns and the

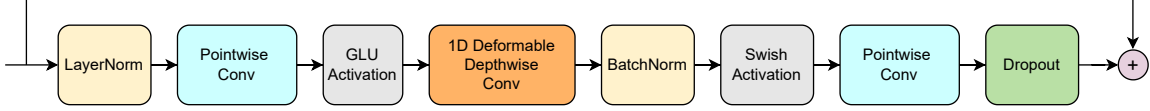


Figure 2: *Deformable convolution module: following the GLU-activated pointwise convolution units, the 1-D depthwise deformable convolution is implemented to replace the regular 1-D depthwise convolution.*

deformation learned. The paper is organized as follows. Sec. 2 discusses related work. Sec. 3 outlines the Deformer encoder design. Sec. 4 presents the analysis of offsets and attention patterns as well as visualizations. Sec. 5 lists the experimental setup and illustrates the results and our findings. Sec. 6 concludes this paper and provides an outlook for future work. We thank our collaborators and acknowledge them in Sec. 7.

2. Related Work

The applications of the deformable CNN focused on areas such as video processing [28] and speaker recognition on the spectrograms [29]. The 1-D deformable CNN was first proposed for action segmentation in [30]. It was only recently that An et al. applied the deformable CNN to speech recognition [27]. In detail, they modified a 7-layer standard TDNN model by making the last several layers deformable. Compared with the base TDNN, the introduction of deformed kernels has shown superior performance on both time-shifted and regular speech. Using neural architecture search, the deformable TDNN achieved a remarkable 10% relative WER improvement on the *eval92* set of WSJ over the base TDNN. Their work designed a system based on the CTC-CRF-based approach [31] to end-to-end (E2E) ASR. Our study here differs by focusing on an encoder design for LAS-based [32] E2E ASR systems, which works with a deep architecture and attention mechanisms.

3. Deformer Encoder

Our proposed Deformer encoder is similar to the Conformer encoder, which has the SpecAug [33], convolution subsampling layers, and stacked attention-convolution blocks. The Deformer uses a deformable convolution module, as depicted in Fig. 2.

3.1. 1-D Deformable Convolution

The 1-D deformable convolution [27] is built on regular convolutions and contains three steps, 1) offset convolution, 2) linear interpolation, and 3) output convolution. The first step uses convolution to predict input position offsets $\Delta p \in \mathbb{R}^{T \times K}$, where T is the input length and K is the kernel size. The prediction uses the initial input positions $p_0 \in \mathbb{R}^{T \times K}$, which are determined by the kernel size, stride, and dilation parameters. These are positions shown green in Fig 1. Given an input sequence X , the first step computes the offset sequence Δp by,

$$\Delta p = \text{Conv1D}_{\text{offset}}(X, p_0). \quad (1)$$

Since the offset values Δp are fractional, the second step will produce a linear interpolation of the input to get corresponding input values at Δp . This procedure is computed by,

$$p' = p_0 + \Delta p, \quad (2)$$

$$X(p') = X(\lfloor p' \rfloor) * (\lfloor p' \rfloor - p' + 1) + X(\lfloor p' \rfloor + 1) * (p' - \lfloor p' \rfloor), \quad (3)$$

where $\lfloor \cdot \rfloor$ is the floor operation and p' is the position sequence after deformation, as shown blue in Fig 1. Lastly, the output convolution is applied to the input at deformed locations. For an output sequence Y , this is computed by,

$$Y = \text{Conv1D}_{\text{output}}(X, p'). \quad (4)$$

Note when Δp is set to zero, we revert back to the regular 1-D convolution that uses the same kernel size, stride, and dilation parameters as which produced the positions p_0 .

3.2. 1-D Deformable Depthwise Convolution

Consider 2-D input $X \in \mathbb{R}^{T \times F}$ with time and frequency information, the depthwise operation slices the input along the F dimension into distinct groups. For a 1-D depthwise convolution, each input slice $X_g \in \mathbb{R}^{T \times F/g}$ is then convolved with a shared weight matrix to produce an output slice $Y_g \in \mathbb{R}^{T \times N/g}$, where N is the output dimension size and g is the number of groups. The idea is that the spatial (T) and channel (F) information of the input can be separated [2]. Since the 1-D deformable convolution deforms the input spatial locations, we make the 1-D depthwise convolution in the Conformer deformable. This means making the $\text{Conv1D}_{\text{output}}$ in Eq. 4 a depthwise operation. It is also intuitive to make the $\text{Conv1D}_{\text{offset}}$ depthwise by setting the *deformable groups*, which removes channel dependencies across groups. However, our empirical result suggests using the same group of offsets for all channels outperforms different groups, as further explained in section 6.2.

4. Pattern Analysis

We conduct a statistical analysis of offset values learned in each deformable layer to interpret deformation. We visualize both localized and global patterns obtained. The spread of attention distribution is evaluated using metrics from [34].

4.1. Setup

The best-performing model on the combined WSJ development and evaluation set is used for analysis. Note we have only used development set in parameter selection. The model contains a 12-layer Deformer encoder and a 6-layer Transformer decoder, predicting the probability of letters. The encoder consists of a mix of deformable and non-deformable CNN layers. Table 1 lists the detailed configurations of our encoder network.

Configurations	Deformable Layers	Non-deformable Layers
Layer Index	{1, 6, 7, 10, 11}	{0, 2-5, 8, 9}
Layer Dimensions	256	256
Attention Heads	4	4
Kernel Size	15	15
Dilation	1	1
Stride	1	1
Convolution Groups	256	256
Deformable Groups	1	1

Table 1: *Deformer Encoder Configuration*

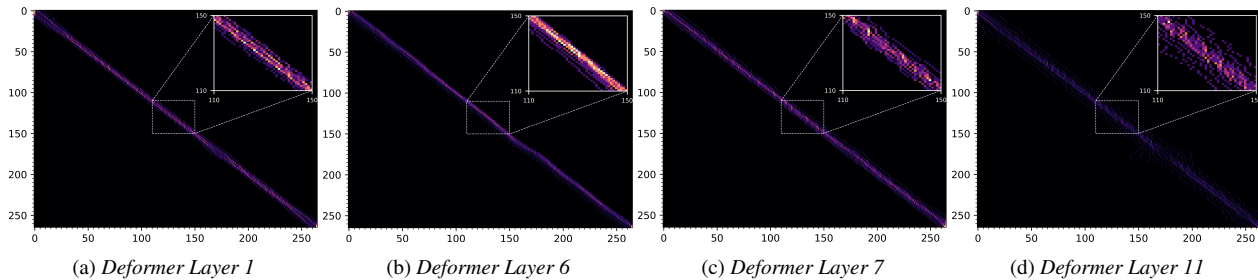


Figure 3: Unrolled convolution locations with deformed kernels on decoding the 4k0c030i utterance. A section is zoomed in and displays a kernel pattern on the upper right corner. The color intensity reflects the number of overlaps at each location (higher the brighter). The horizontal axis shows the input positions and the vertical axis shows the output positions.

4.2. Localized Patterns and Offset Statistics

Fig. 3 unrolls the deformable convolution and visualizes the learned receptive fields of kernels after the offset. From the utterance perspective, the network learns to place kernels along the diagonal, which affirms a monotonic alignment is optimal for speech recognition. In each row, the receptive field of a kernel does not show a large deviation from the local context even though we do not limit the magnitude for offsets (except to the boundaries of the utterance). Hence, localized patterns are beneficial overall despite a few exceptions in deep layers (e.g. positions from (165,165) to (185,185) in Fig. 5d). It is worth noting that the addition of offset can make several positions *overlap*. By observing the overlaps, we conclude a concentration pattern adopted by the network. The center of a kernel has a high focus on the local information, which shows typically bright-colored. The sides of a kernel scatter to distant information that is only supportive, which appear light-colored. Thus, we think the deformable CNN constructs meaningful features by shifting to locations where it helps enhance a locally present knowledge.

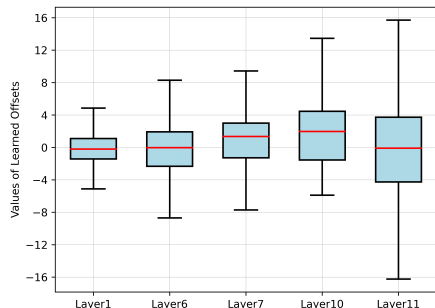


Figure 4: Boxplots of offset distribution in each deformable layer on the combined dev93 and eval92 set. The box boundaries are the first (Q1) and the third quartiles (Q3). The red line is the median. The whiskers denotes values within a 1.5 times interquartile range below Q1 and above Q3.

Since offset values change with different input, Fig. 4 displays the distributions of offsets collected on the corpus level. We first observe a larger receptive field obtained in deeper layers, shown by an increasing spread of the distribution. Next, we confirm the concentration pattern persists across different utterances (as previously discussed on a single utterance). Each set of Q1 and Q3 values in Layers 1, 6, and 11 is nearly symmetric around the zero medians. This explains the deformation around the kernel center because the focus (overlap) requires shifting nearby positions either to its past or future. The distributions also present a long tail. This explains the deformation of the kernel sides, where supporting information is afar and scattered.

4.3. Global Pattern

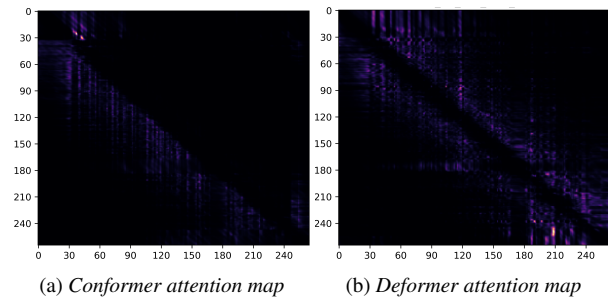


Figure 5: Attention maps obtained by the last layer of the Conformer and Deformer for the 4k0c030i utterance. Output is on the vertical axis that attends to input on the horizontal axis.

Fig. 5 compares attention maps obtained by the last layer of the Conformer and the Deformer encoder for a single utterance. From the graphs, we may speculate that both provide associations to the representations on the diagonal. The Conformer attends only to the past except for the first 30 locations where no history exists. But the Deformer attends additionally to the future above the diagonal. This may indicate deformed local features induce more global relevance than regular features.

Model	Globalness (0, 7.48]	Verticality [-7.48, 0]	Diagonality [-0.75, 0]
Conformer	4.57	-6.95	-0.18
Deformer	4.82	-6.97	-0.19

Table 2: Quality evaluation of the attention heads.

To verify our observation, we evaluate the spread of attention for each head using the metrics in [34] and report the average value across all heads on the combined set. The globalness measures the average entropy of attention distributions (an overall spread). The verticality measures the entropy of averaged attention distribution (a vertical spread). The diagonality measures the diagonal spread that helps obtain speech alignments [35] and achieves maximum at zero when the attention is on the main diagonal. For all metrics, a larger score indicates more spread. Note the bounds of all metrics depend on lengths of the encoded sequences in the corpus, which we calculate and include in Table 2. It shows attention obtained by the Deformer indeed has an increase in global spread, which verifies the boost of overall feature associations led by deformation. Based on the metrics, we know that a random increase in attention globally can cause a severe decrease in both verticality and diagonality.

But in the range of each respective bounds, we observe less significant decreases in both metrics compared to the increase in globalness (-0.3% or -1.3% vs. $+3.3\%$), indicating the Deformer boosts feature associations while retaining the original attention structure such as the diagonals shown in Fig. 5b.

5. Experiments

The experiments are conducted on the Wall Street Journal (WSJ) corpus using recipes from the Espnet toolkit [36]. WSJ [37] is a standard benchmark dataset to evaluate speech recognition system performance. The WSJ dataset includes read speech with transcripts drawn from the newspaper. The data is partitioned into 81 hours of training speech (*si284*), 1 hour for development (*dev93*), and 0.7 hour for evaluation (*eval92*). The average utterance length is 7.8 seconds. Except for the SpecAug, we do not utilize any data augmentation methods.

5.1. Baseline System

Our baseline for WSJ follows the identical setup provided in the Espnet except for the batch size and GPUs. The model has a 12-layer Conformer encoder and a 6-layer Transformer decoder. The model dimension is 256 and has 4 attention heads. The system is trained based on English letters by the joint ctc-attention loss with a ctc weight of 0.3. The Adam [38] optimizer is used with a warmup learning scheduler, setting $lr_peak = 0.005$ and $warmup_steps = 30,000$. We use two GPUs with 1.25M elements in each batch. Unless stated otherwise, these hyperparameters are kept the same in the following experiments.

5.2. The Deformer Encoder Layer Setup

The Deformer encoder has a default setup with deformable layers at 1, 6, 7, 10, and 11. A learning rate multiplier is commonly set for the offset CNN to learn in different rates than the rest of the model. We find both multipliers $mult = 0.5$ and 1.0 work better and report the results with these settings below.

5.2.1. Parameter Initialization

The parameter initialization is crucial to training the Deformer encoder. It is common to start parameters of the offset CNN from zero for the deformable CNN. But the overall parameters of the model are initialized by the Xavier [39] method. We test and compare these two initialization strategies under varying learning rate multipliers, denoted by 1) *Xavier*: all parameters are initialized by Xavier, 2) *Zero*: all parameters are initialized by Xavier except the offset CNN is initialized to zero.

Model	#Params	Initialization	WER (%)		CER (%)	
			dev	eval	dev	eval
Conformer Base	43.05M	Xavier	11.2	8.9	3.9	3.0
Deformer ($mult=0.5$)	43.34M	Xavier	10.7	8.4	3.7	2.8
Deformer ($mult=1.0$)	43.34M	Xavier	11.1	9.0	3.9	3.0
Deformer ($mult=0.5$)	43.34M	Zero	10.8	8.8	3.7	3.0
Deformer ($mult=1.0$)	43.34M	Zero	10.5	8.4	3.7	2.9

Table 3: WERs and CERs of using different parameter initialization schemes for the Deformer.

As shown in Table 3, both methods can result in the best WER of 8.4% on the evaluation set, which improves the Conformer baseline by a +5.6% relative. The systems use different learning rate multipliers, which indicates the architecture can be sensitive to this hyperparameter. Tying all deformable layers with a single learning rate multiplier may have magnified its impact. However, the Deformer initialized by the *Zero* setup has

a smaller change in WERs across different learning rate multipliers comparing the *Xavier* initialization. It has also outperformed the baseline in both setups. Hence, we conclude that it is beneficial to use the *Zero* setup for the Deformer.

5.2.2. Deformable Groups

Model	Deformable Groups	WER (%)		CER (%)	
		dev	eval	dev	eval
Deformer ($mult=0.5, zero\ init.$)	256	11.2	9.1	3.9	3.0
Deformer ($mult=1.0, zero\ init.$)	256	11.1	8.9	3.9	3.0
Deformer ($mult=0.5, zero\ init.$)	2	11.1	8.6	3.8	2.9
Deformer ($mult=1.0, zero\ init.$)	2	10.9	8.6	3.9	2.8
Deformer ($mult=0.5, zero\ init.$)	1	10.8	8.8	3.7	3.0
Deformer ($mult=1.0, zero\ init.$)	1	10.5	8.4	3.7	2.9

Table 4: WERs and CERs of using different number of offset groups

As previously stated in Sec. 3.2, making the offset CNN a depthwise operation is still debatable. We experimented extensively with 1, 2, and 256 deformable groups under varying learning rate multipliers. As shown in Table 4, the model performs better on both the development and evaluation set when the number of offset groups reduces. We suspect it is reasonable since the small number of offset groups should help the deformable layer discover localized patterns that are general. Moreover, the potential impact of having channel dependencies on the offset output is probably very small.

5.2.3. Language Model

Model	WER (%)		CER (%)	
	dev	eval	dev	eval
Conformer Base	7.0	4.7	3.1	2.1
Deformer ($mult=1.0, zero\ init.$)	6.7	4.4	2.9	2.0

Table 5: Conformer vs. Deformer on WSJ (LM weight=1.0)

Finally, we investigate whether the improvement found in the encoder can persist after adding an external language model. In detail, we use a pre-trained transformer language model and balance the decoding scores using a LM weight of 1.0. As shown in Table 5, the Deformer outperforms the Conformer baseline across the table, with a notable +6.7% WER improvement on the WSJ *eval92* set.

6. Conclusions & Future Work

In conclusion, we present a novel encoder design for end-to-end speech recognition. It is shown that the Deformer encoder strengthens localized patterns by deforming convolutional kernels to focus on task-relevant regions, which further enhances attention mechanisms. On the WSJ evaluation dataset, the Deformer achieves a notable +6.4% relative WER improvement over the Conformer model. We notice the system can be sensitive to the learning rate multiplier due to layer tying and verify in experiments that using zero initialization for the offset CNNs and MVN for the input alleviate such issues and increase robustness. For future work, we want to improve the model robustness more, for which the solution can lead to a larger model design and exploration for more deformable layers.

7. Acknowledgements

The authors would like to thank Wei Xia and Szu-Jui Chen for their meaningful discussion and suggestions on the work.

8. References

- [1] A. Krizhevsky, I. Sutskever, and G. E. Hinton, "Imagenet classification with deep convolutional neural networks," *Advances in Neural Info. Proc. Systems*, vol. 25, 2012.
- [2] F. Chollet, "Xception: Deep learning with depthwise separable convolutions," in *Proceedings of the IEEE conference on computer vision and pattern recognition*, 2017, pp. 1251–1258.
- [3] K. He, X. Zhang, S. Ren, and J. Sun, "Deep residual learning for image recognition," in *Proceedings of the IEEE conference on computer vision and pattern recognition*, 2016, pp. 770–778.
- [4] J. Gehring, M. Auli, D. Grangier, and Y. Dauphin, "A convolutional encoder model for neural machine translation," in *Proc. of the 55th Annual Meeting of the Assoc. for Computational Linguistics*, Jul. 2017, pp. 123–135.
- [5] A. Conneau, H. Schwenk, L. Barrault, and Y. Lecun, "Very deep convolutional networks for text classification," in *Proc. of the 15th Conf. of the Europ. Chapter of the Assoc. for Computational Linguistics*, Apr. 2017.
- [6] Z.-H. Jiang, W. Yu, D. Zhou, Y. Chen, J. Feng, and S. Yan, "Convbert: Improving bert with span-based dynamic convolution," *Advances in Neural Info. Proc. Systems*, vol. 33, pp. 12 837–12 848, 2020.
- [7] H. Zhang, I. McLoughlin, and Y. Song, "Robust sound event recognition using convolutional neural networks," in *IEEE ICASSP-15*, pp. 559–563.
- [8] L.-C. Yang, S.-Y. Chou, and Y.-H. Yang, "Midinet: A convolutional generative adversarial network for symbolic-domain music generation," *arXiv:1703.10847*, 2017.
- [9] V. K. Kothapally and J. H. Hansen, "Skipconvgan: Monaural speech dereverberation using generative adversarial networks via complex time-frequency masking," *IEEE/ACM Transactions on Audio, Speech, and Language Processing*, 2022.
- [10] D. Dimitriadis, P. Maragos, and A. Potamianos, "Robust am-fm features for speech recognition," *IEEE Signal Proc. Letters*, vol. 12, no. 9, pp. 621–624, 2005.
- [11] C. J. Long and S. Datta, "Wavelet based feature extraction for phoneme recognition," in *IEEE ICSP-96*, vol. 1, pp. 264–267.
- [12] Y. Chen, X. Dai, M. Liu, D. Chen, L. Yuan, and Z. Liu, "Dynamic convolution: Attention over convolution kernels," in *Proceedings of the IEEE/CVF Conference on Computer Vision and Pattern Recognition*, 2020, pp. 11 030–11 039.
- [13] J. Hu, L. Shen, and G. Sun, "Squeeze-and-excitation networks," in *Proceedings of the IEEE conference on computer vision and pattern recognition*, 2018, pp. 7132–7141.
- [14] R. Riad, O. Teboul, D. Grangier, and N. Zeghidour, "Learning strides in convolutional neural networks," *CoRR*, vol. abs/2202.01653, 2022.
- [15] P. v. Platen, C. Zhang, and P. Woodland, "Multi-span acoustic modelling using raw waveform signals," *Interspeech 2019*.
- [16] K. J. Han, J. Pan, V. K. N. Tadala, T. Ma, and D. Povey, "Multistream cnn for robust acoustic modeling," in *IEEE ICASSP-21*, pp. 6873–6877.
- [17] Y. Zhang, W. Chan, and N. Jaitly, "Very deep convolutional networks for end-to-end speech recognition," in *IEEE ICASSP-17*, pp. 4845–4849.
- [18] L. Lu, C. Liu, J. Li, and Y. Gong, "Exploring transformers for large-scale speech recognition," *arXiv:2005.09684*, 2020.
- [19] R. Li, X. Wang, S. H. Mallidi, S. Watanabe, T. Hori, and H. Hermansky, "Multi-stream end-to-end speech recognition," *IEEE/ACM Transactions on Audio, Speech, and Language Processing*, vol. 28, pp. 646–655, 2019.
- [20] S. Kriman, S. Beliaev, B. Ginsburg, J. Huang, O. Kuchaiev, V. Lavrukhin, R. Leary, J. Li, and Y. Zhang, "Quartznet: Deep automatic speech recognition with 1d time-channel separable convolutions," in *IEEE ICASSP-20*, pp. 6124–6128.
- [21] W. Han, Z. Zhang, Y. Zhang, J. Yu, C.-C. Chiu, J. Qin, A. Gulati, R. Pang, and Y. Wu, "Contextnet: Improving convolutional neural networks for automatic speech recognition with global context," *Interspeech 2020*.
- [22] A. Gulati, J. Qin, C.-C. Chiu, N. Parmar, Y. Zhang, J. Yu, W. Han, S. Wang, Z. Zhang, Y. Wu *et al.*, "Conformer: Convolution-augmented transformer for speech recognition," *Interspeech 2020*.
- [23] A. Vaswani, N. Shazeer, N. Parmar, J. Uszkoreit, L. Jones, A. N. Gomez, Ł. Kaiser, and I. Polosukhin, "Attention is all you need," *Advances in Neural Info. Proc. Systems*, vol. 30, 2017.
- [24] S. Chen, Y. Wu, Z. Chen, J. Wu, J. Li, T. Yoshioka, C. Wang, S. Liu, and M. Zhou, "Continuous speech separation with conformer," in *IEEE ICASSP-21*, pp. 5749–5753.
- [25] P. Ma, S. Petridis, and M. Pantic, "End-to-end audio-visual speech recognition with conformers," in *IEEE ICASSP-21*, pp. 7613–7617.
- [26] J. Dai, H. Qi, Y. Xiong, Y. Li, G. Zhang, H. Hu, and Y. Wei, "Deformable convolutional networks," in *IEEE Inter. Conf. on Comp. Vision*, 2017, pp. 764–773.
- [27] K. An, Y. Zhang, and Z. Ou, "Deformable tdnn with adaptive receptive fields for speech recognition," *Interspeech 2021*.
- [28] X. Xu, M. Li, and W. Sun, "Learning deformable kernels for image and video denoising," *arXiv:1904.06903*, 2019.
- [29] Y. Zhang, H. Yu, and Z. Ma, "Speaker verification system based on deformable cnn and time-frequency attention," in *IEEE Asia-Pacific Signal and Info. Proc. Conf. (APSIPA ASC)*, pp. 1689–1692.
- [30] P. Lei and S. Todorovic, "Temporal deformable residual networks for action segmentation in videos," in *Proceedings of the IEEE conference on computer vision and pattern recognition*, 2018, pp. 6742–6751.
- [31] H. Xiang and Z. Ou, "Crf-based single-stage acoustic modeling with ctc topology," in *IEEE ICASSP-19*, pp. 5676–5680.
- [32] W. Chan, N. Jaitly, Q. Le, and O. Vinyals, "Listen, attend and spell: A neural network for large vocabulary conversational speech recognition," in *IEEE ICASSP-2016*, pp. 4960–4964.
- [33] D. S. Park, W. Chan, Y. Zhang, C.-C. Chiu, B. Zoph, E. D. Cubuk, and Q. V. Le, "SpecAugment: A simple data augmentation method for automatic speech recognition," *arXiv:1904.08779*, 2019.
- [34] S.-w. Yang, A. T. Liu, and H.-y. Lee, "Understanding self-attention of self-supervised audio transformers," *Interspeech 2020*.
- [35] S. Kim, T. Hori, and S. Watanabe, "Joint ctc-attention based end-to-end speech recognition using multi-task learning," in *IEEE ICASSP-17*, pp. 4835–4839.
- [36] S. Watanabe, T. Hori, S. Karita, T. Hayashi, J. Nishitoba, Y. Unno, N. E. Y. Soplin, J. Heymann, M. Wiesner, N. Chen *et al.*, "Espnet: End-to-end speech processing toolkit," *arXiv:1804.00015*, 2018.
- [37] D. B. Paul and J. Baker, "The design for the wall street journal-based csr corpus," in *Speech and Natural Language: Proceedings of a Workshop Held at Harriman, New York, February 23-26, 1992*, 1992.
- [38] D. P. Kingma and J. Ba, "Adam: A method for stochastic optimization," in *3rd International Conference on Learning Representations, ICLR 2015, Conference Track Proceedings*, 2015.
- [39] X. Glorot and Y. Bengio, "Understanding the difficulty of training deep feedforward neural networks," in *Proceedings of the thirteenth international conference on artificial intelligence and statistics. JMLR Workshop and Conference Proceedings*, 2010, pp. 249–256.